Pergamon

Int. J. Heat Mass Transfer. Vol. 40, No. 10, pp. 2431–2443, 1997

0017–9310/97 $17.00+0.00

PII: S0017–9310(96)00270–0

Experimental mass (heat) transfer in and near a circular hole in a flat plate

H. H. CHO
Department of Mechanical Engineering, Yonsei University, Seoul 120-749, Korea

M. Y. JABBARI
Department of Mechanical Engineering, Saginaw Valley State University, University Center, MI 48710, U.S.A.

and

R. J. GOLDSTEIN†
Department of Mechanical Engineering, University of Minnesota, Minneapolis, MN 55455, U.S.A.

(*Received* 30 *August* 1995 *and in final form* 15 *July* 1996)

Abstract—Experiments are performed to investigate the local heat/mass transfer characteristics for flow through a single circular hole in a thin perforated plate (modeling a combustor wall). The naphthalene sublimation technique is employed to determine the local values on the hole's inner surface and in the vicinity of the hole entrance and exit. The hole-length-to-diameter ratio varies from 0.5 to 1.5, and the ratio of the diameter of the outer boundary (active area) to the hole diameter varies from 1.5 to 4.5. The Reynolds number based on the hole diameter is between 600 and 30 000. On the windward surface, the heat/mass transfer coefficient increases rapidly as the flow approaches the hole entrance due to flow acceleration with a thin boundary layer. Inside the hole, a separation zone at the hole entrance decreases with increasing Reynolds number and then remains constant, approximately 0.56 hole diameter in depth, as the Reynolds number is increased further. The mass transfer coefficient at the reattachment point is about four times that for fully-developed tube flow. The mass transfer variations indicate a laminar separation and a turbulent reattachment flow in this Reynolds number range. The transfer coefficient on the leeward surface is small for the single hole flow because of a weak entrainment-flow velocity. The overall transfer rate is dominated by the inside hole surface (approximately 60%) in spite of its small surface area. Correlations are proposed for local/average heat transfer in short single holes as a function of Reynolds numbers and hole aspect ratios.

INTRODUCTION

Knowledge of local heat transfer coefficients in and around a short hole is necessary for the successful design of film cooling holes of turbine blades and combustor walls. Film cooling is often used to protect surfaces from hot gases in components of high-performance gas turbine engines. The thermal efficiency and specific power of gas turbine systems depend strongly on turbine inlet temperature. Inlet temperature is limited by the potential structural failure of engine components at high temperature. Total coverage cooling has been developed for some components, notably the combustion chamber. This cooling scheme helps to prevent thermal stresses and permits increased efficiency. With total coverage cooling, the analysis of overall heat transfer requires heat transfer coefficients around the hole entrance and inside the hole surfaces as well as adiabatic wall temperature (film cooling effectiveness) on the exposed surfaces.

Present study investigates heat/mass transfer for flow through short single circular holes in a flat wall. Flow in a single hole closely approximates the flow through arrays of holes (total coverage cooling) with a large hole-to-hole spacing [1]. Cho and Goldstein [2] showed that heat/mass transfer on the inner hole surface is not greatly affected by a cross-flow at the hole exit in a large range of blowing rates. They also found that heat transfer coefficients on hole entrance surfaces (windward or backside of cooling walls) are the same with and without cross-flows at the hole exit. Thus, the local mass transfer coefficients obtained in this study can be used in predicting film cooling in gas turbine blades and combustor walls. The mass transfer data obtained on the leeward (exposed) surface cannot be used directly in predicting film cooling as there is no cross-flow. However, the information on this surface is valuable in an analysis of conduction effects of walls in heat transfer experiments. The transfer coefficient on the surface at the hole exit also models

† Author to whom correspondence should be addressed.

NOMENCLATURE

d diameter
d_h hydraulic diameter of an annulus ($=d_o-d_i$)
d_i hole diameter ($12.6\text{ mm} \leqslant d_i \leqslant 38.1\text{ mm}$)
d_o diameter of outer (active) boundary on windward and leeward surfaces ($1.5 \leqslant d_o/d_i \leqslant 4.5$)
D_{naph} mass diffusion coefficient of naphthalene vapor in air
h_m local mass transfer coefficient, equation (1)
l distance from the outer (active) boundary
L dimensionless length ($=Y/d_i$)
L' dimensionless length ($=Y/Y_{peak}$)
$\dot{m}$ local naphthalene mass transfer rate per unit area
Nu_∞ Nusselt number for a fully developed circular tube flow
Pr Prandtl number
Re Reynolds number based on the hole diameter and the average velocity in a hole
Sc Schmidt number for naphthalene in air, ν/D_{naph}; about 2.28 at 298 K and 0.1 MPa
Sh local Sherwood number based on the hole diameter, equation (2)
Sh_{dh} local Sh based on the hydraulic diameter d_h; $h_m d_h/D_{naph}$
Sh_{do} local Sh based on the outer (active) boundary diameter d_o; $h_m d_o/D_{naph}$
Sh_L cumulatively-averaged Sherwood number (averaged from the hole entrance to the position, L); $\int_0^L Sh\,dy/L$
Sh_{peak} local peak Sh in hole
Sh_∞ reference Sherwood number for a fully developed circular tube flow
$\overline{Sh}$ average Sherwood number; $\iint Sh\,d\theta\,dy / \iint d\theta\,dy$ for hole and $\iint Sh\,dx\,dz / \iint dx\,dz$ for plate
$\overline{Sh}_{dh}$ average Sherwood number based on the hydraulic diameter d_h
$\overline{\overline{Sh}}$ overall-averaged Sherwood number; $(\iint Sh\,d\theta\,dy + \iint Sh\,dx\,dz)/(\iint d\theta\,dy + \iint dx\,dz)$
$\overline{\overline{Sh}}_{do}$ overall-averaged Sherwood number based on the outer (active) boundary diameter
t hole length ($0.5 \leqslant t/d_i \leqslant 1.5$)
T_w local wall temperature
X, Z distance from the center of a hole (Cartesian coordinates in Fig. 2)
Y coordinates and direction along the hole axis
Y_{peak} peak Sh location inside the hole (reattachment point).

Greek symbols
$\delta\tau$ test duration
δz local sublimation depth of naphthalene
ρ_s density of solid naphthalene
$\rho_{v,w}$ naphthalene vapor density at the surface
$\rho_{v,\infty}$ naphthalene vapor density of the approaching flow ($\rho_{v,\infty} = 0$ in the present study)
θ angle around hole.

heat transfer problems around jet nozzle exits. The literature shows little research on heat transfer in a short hole due to the inherent measurement difficulties.

In heat transfer experiments, it is difficult to measure the local heat transfer rate near the hole and inside the hole surface. Such measurement includes a large conduction error resulting from sharp temperature gradients around the hole entrance. A mass transfer technique can be used to measure transfer rates on the inside hole surface and on the plate around the hole entrance and the hole exit. The mass transfer experiment excludes conduction in the solid wall and gives finer spatial resolution of transfer coefficients. The detailed local heat/mass transfer measurements in the hole and around the hole entrance are essential to verify the use of advanced computational methods to predict film cooling performance. The mass transfer measurements can be converted to heat transfer results using the heat/mass transfer analogy.

The local mass transfer rates are obtained from the test plate cast with naphthalene around the hole and inside the hole. The naphthalene sublimation method is a well-known mass transfer technique. The surface boundary condition is analogous to an isothermal surface in a corresponding heat transfer situation. Concentration gradients and the mass flux are analogous to temperature gradients and the heat flux. The time average local mass transfer rates are obtained from measurements of the sublimation depths. Although the mass transfer coefficient is obtained with a constant vapor pressure at the wall (equivalent to isothermal boundary condition), it can often be

applied to other boundary conditions because the heat/mass transfer coefficient is usually a weak function of the wall temperature distribution in turbulent flows.

There are few publications concerning the geometry studied herein. Gurdal [3] measured the overall-averaged mass transfer rates for an upstream-facing (windward) surface using a weighing method for cast naphthalene. The diameter ratios of the outer boundary (active area) to the hole were 6–14.4 and the Reynolds number, based on the outer boundary diameter, was varied from 200 to 3000. He found that Sh_{do} was proportional to Reynolds number to the power of 0.452 and the data correlated well with the characteristic length of the outer diameters.

Lichtarowicz *et al.* [4] investigated discharge coefficients and pressure distributions for flow through thick orifices in a pipe line. The ratios of the orifice thickness to the orifice diameter were from 0.5 to 10 and Reynolds number was varied from 10 to 10^5. They determined that the separation length changes significantly with transitional or turbulent flows in the hole and the pressure recovery depends greatly upon whether or not there is reattachment. Flow characteristics play a key role in the heat transfer distribution.

For long tubes, Boelter *et al.* [5], Mills [6], Petukhov [7], Al-Arabi [8], and Lloyd and Brown [9] studied heat transfer rates in the entrance region of circular tubes. The closest data to the entrance was generally about 0.5 diameter downstream and the results vary greatly among the references.

Operating conditions

We found no published literature for the local transfer coefficients, which are essential in design and analysis, for flow through short holes. The present study deals with the local transfer rates for the hole-length-to-diameter ratios of 0.5–1.5 (18.9–37.6 mm) and for the diameter ratios of the outer boundary (active area) to the hole of 1.5–4.5. The hole diameters are varied from 12.6 to 38.1 mm. The employed Reynolds numbers based on the hole diameter are in a range of 100–30 000. This Reynolds number range includes the operating condition in an actual film cooling of turbine blades and combustor walls. The lower Reynolds numbers are essential to simulate flow through laminate plates with perforations but are restricted by measurement difficulties, such as natural convection effects.

EXPERIMENTAL APPARATUS AND PROCEDURE

Suction plenum chamber

Cho [1] describes the experimental apparatus in detail. A brief description is included here. An active area of test piece is positioned at the center of a plenum's top wall and is mounted flush with the non-active section of the wall. The plenum chamber has a square cross-section (572 by 572 mm) and a height

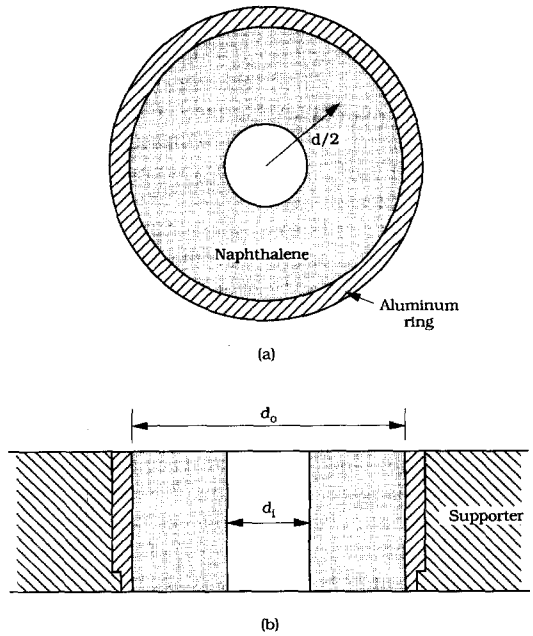

Fig. 1. Test plate for weighing measurements: (a) plain view; (b) cross-sectional view.

of 1400 mm. A settling baffle around the chamber essentially eliminates the influence of random motions of room air. It has openings at the top and around the plenum chamber at its bottom. The openings of the settling baffle are covered with screens (meshes) and cloth to break down eddies in the incoming air flow. Room air drawn into the settling baffle passes through the perforated test plate into the plenum chamber, through the orifice plate (flow measuring device) and the blower and then is discharged outside the building.

Test plates and naphthalene casting procedure

The experimental facility enables measurement of the local/average naphthalene sublimation rates on the inside hole surface and on the surfaces near the hole which are exposed to an air flow. The test plates are cast with a thin naphthalene layer for sublimation prior to being exposed to the air stream. Two different types of test specimen are used in the present experiments: one for average (weighing) measurements and local values on windward and leeward surfaces; the other for local measurements on inside hole surfaces.

For average (weighing) measurements, small annular naphthalene test specimens are employed as shown in Fig. 1. The inner diameter of the hole and the outer boundary (active area) are varied during the course of the experiments. The hole diameters ranged from 12.6 to 38.1 mm while the ratio of the hole-length-to-diameter and the diameter ratio of the outer boundary to the hole varied from 0.5 to 1.5 and 1.5 to 4.5, respectively. Local measurements on the windward and leeward surfaces are also conducted on the small hole plates. To accommodate a mass limitation of 200 g for the laboratory balance, the test plates are

machined thin to reduce the total mass. The test plates have only an aluminum outer ring, the entire inside annulus is cast naphthalene. For other weighing experiments, selected active surfaces are covered with an aluminum sheet and/or tube to measure individual average mass transfer rates. For example, the inside hole and leeward surfaces were covered to measure the average windward surface mass transfer. The short measurement time possible with the weighing experiment reduces greatly extraneous natural convection effects. This average (weighing) measurement is compared with an average determined from the local measurement results.

For local mass transfer rate measurements in a hole, a special test specimen (Fig. 2) is fabricated. The plate is an aluminum block pierced at its center by a hole of 25.4 mm diameter. In addition, the test plate contains a recess into which naphthalene can be cast. A square outer boundary (active area) of the windward and leeward surfaces simulates a section within an array of holes. The square cavity 101.6 mm ($4d_i$) by 101.6 mm ($4d_i$) is machined around the hole of the test plate on the windward and leeward surfaces. This becomes the naphthalene surface after casting. The rim around the naphthalene cast plate provides a surface on which measurement reference points are located. The hole (25.4 mm diameter) is recessed about 3.2 mm deep. During casting, this recess is filled with naphthalene and the 25.4 mm diameter circular hole is formed. The hole has metal annular rims with thicknesses of 1.0 mm at the top and 1.5 mm at the bottom which are exposed to the airflow. The rims of the hole, which are nonsubliming surfaces, are used as reference points for inside-hole measurements. Additional grooves, which roughen the recess area, aid adhesion of naphthalene to the plate.

The naphthalene surfaces employed in the experiments are cast. The mold consists of the test plate, a highly polished aluminum flat plate and a circular cylinder (polished using aluminum powder grade no. 3). Molten naphthalene (near boiling point) is poured into the mold. Each mold has vent holes for the air displaced by the molten naphthalene. After the naphthalene solidifies and cools to room temperature, the molds are separated from the test piece by applying a shear force. The smoothness of the exposed naphthalene surface is comparable to that of the polished aluminum adjacent to it.

Data acquisition system

A computer controled measurement system is used to scan the profile of the naphthalene surface. This system satisfies many requirements to obtain useful local sublimation depths of a naphthalene surface. These include precise positioning of the plates, accurate depth measuring and rapid data acquisition to minimize the natural convection losses. Two different computer-controled measurement systems, an XY-table and a four-axis table, are used for the flat plate measurement and the inside hole measurement, respectively. The four-axis table is similar to the XY-table, but its two additional degrees of freedom allows more flexibility in the geometries that it can accommodate such as the inside-hole measurement.

The measurement system [10] includes a depth gauge, a linear signal conditioner, a digital multimeter, stepper-motor driven positioners, a motor controler and a microcomputer. With this automated system one can obtain about two thousand data points in 1 h.

The depth gauge (a linear variable differential transformer; LVDT) has a 0.5 mm linear range and 25 nm (1.0 μin) resolution. The nominal sublimation depth in a test is around 50 μm (2 mil), about three orders of magnitude larger than the resolution. The linearity of the LVDT is within 0.1% of the measuring range. To measure inside hole mass transfer rates, an extended stylus is used to reach deep inside the hole [1]. The 50.8 mm long stylus is set at a 60° angle from the moving direction of the sensor. A carbide ball of 1.588 mm diameter at the tip is used to minimize the scratches on the naphthalene surface and still provide reasonable sensing of slope changes. The measurement errors of the LVDT are about 0.15 μm (6 μin) for the flat plate measurement and about 0.45 μm (18 μin) for the inside hole measurement at a 95% confidence level.

Measurements

The profile of the naphthalene surface is determined before and after each test run. The difference between the two sets of surface elevations (with respect to reference positions on the nonsubliming metal surface) is a measure of the sublimation depth. Each test run time is selected so that the average sublimation depth of the naphthalene surface will be about 0.05 mm (0.002 in). The sublimation depth is two or three orders of magnitude higher than the measurement error. The maximum sublimation depth, $\sim$ 0.2 mm, is about 0.8% of the nominal hole diameter of 25.4 mm.

For the small plates, a weighing method is used to determine the overall-averaged mass transfer rate. This method, using a precision balance, has a smaller measurement error and little natural convection loss during the measurement, because it can be conducted quickly. The balance, a Sartorius analytical balance, has a resolution of 0.1 mg and a capacity of 200 g. The overall-averaged Sherwood numbers from the weighing measurement compare well with numerically integrated values from local measurements.

Because the vapor pressure of naphthalene is quite sensitive to temperature (about 10% change per °C), the naphthalene surface temperature is measured using T-type (copper-constantan) thermocouples installed within the naphthalene, as close as possible to the surface. During the run, the temperature variation of the naphthalene surface is maintained within about 0.2°C.

The local mass transfer coefficient,

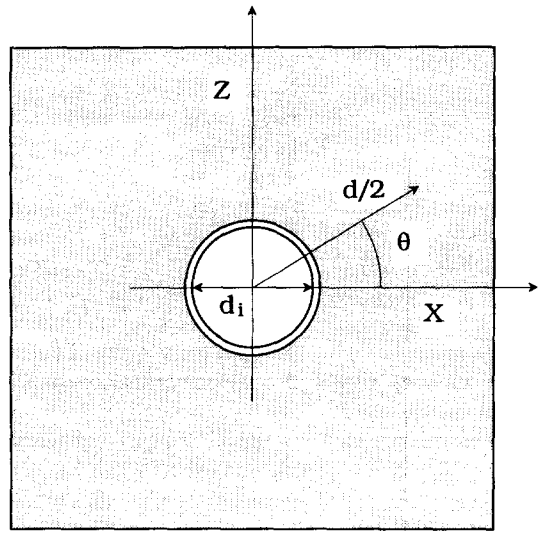

(a)

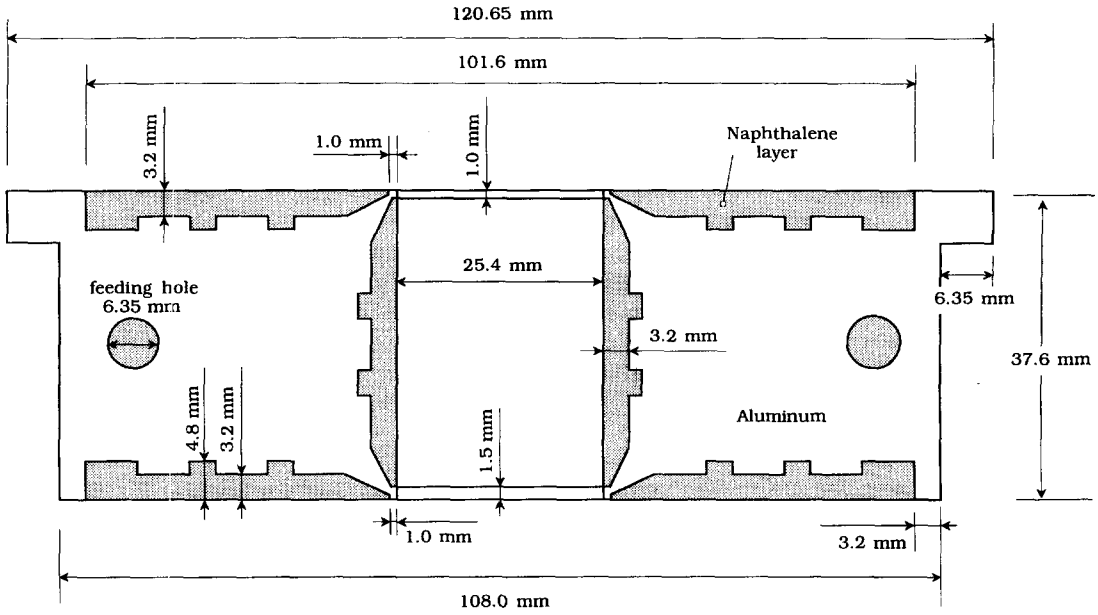

(b)

Fig. 2. Test plate for the inside hole measurements: (a) coordinate system; (b) cross-sectional view.

$$h_m = \frac{\dot{m}}{\rho_{v,w} - \rho_{v,\infty}} = \frac{\rho_s \delta z/\delta \tau}{\rho_{v,w}} \quad (1)$$

since $\rho_{v,\infty} = 0$ in the present study. The Sherwood number can be expressed as;

$$Sh = \frac{h_m d_i}{D_{naph}} \quad (2)$$

The naphthalene vapor pressure, obtained from a correlation of Ambrose *et al.* [11], is used in calculating the naphthalene vapor density, $\rho_{v,w}$, from the perfect gas law. D_{naph} is determined from a correlation recommended by Goldstein and Cho [10]. Sublimation losses by natural convection are subtracted from the total sublimation.

The uncertainty of the Sherwood numbers, found using Kline and McClintock's [12] method for single sample experiments and considering the measured temperature, depth, position and correlation equations, is within 7.1% for the entire operating range of the measurements based on a 95% confidence level. This uncertainty is mainly attributed to the uncertainty in the properties of naphthalene, such as the naphthalene saturated vapor pressure (3.77%) and diffusion coefficient of naphthalene vapor in air (5.1%). In contrast, the error due to the depth

measurement is only 0.9%. The other uncertainties are 0.1, 1.1 and 4.9% for T_w, ρ_s and h_m, respectively.

RESULTS AND DISCUSSIONS

When a fluid approaches a hole, such as in sink flow (acceleration to the hole), it washes an upstream-facing (windward) surface as shown schematically in Fig. 3. The flow boundary layer, developed far away, thins out as it approaches the hole due to rapid flow acceleration. With the thin boundary layer, a high heat/mass transfer rate is expected to occur near the hole. The flow may separate at the inlet (sharp-edged) of the hole and subsequently reattach inside the hole. This results in a large variation of the heat/mass transfer rate. The heat transfer rate is low within the separation region due to the low wall velocity and because fluid is trapped in the recirculation bubble. The heat transfer then increases quickly downstream and has a maximum value in the reattachment region. Then, the heat transfer rate decreases gradually downstream, as in developing pipe flow. The flow leaving the hole induces an entrained flow on the downstream-facing (leeward) surface which, however, has much lower velocities than does the exit flow.

Windward and leeward surfaces

On the windward surface, the approaching flow is essentially a sink flow. The active area, which is coated by naphthalene and corresponds to an isothermal boundary condition in heat transfer, is an annular area defined by diameters, d_i and d_o (Fig. 1). The mass transfer is high at the outer edge with the startup of the mass transfer boundary layer. The mass transfer coefficient decreases with d and stays relatively uniform till the flow approaches the hole. Most of this middle region has near-uniform transfer coefficient because the growth of the concentration boundary layer is suppressed by acceleration of the flow.

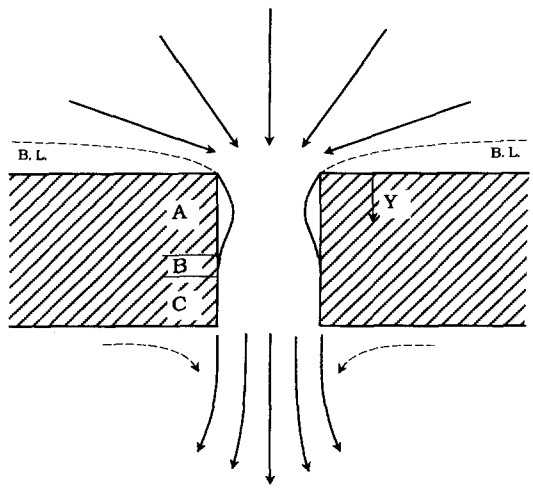

Fig. 3. Schematic flow pattern through a hole.

However, the transfer coefficients increase rapidly near the inlet of the hole due to the thinning of the boundary layer. On the leeward surface, an entrained flow washes into the exit jet stream. The entrained flow velocity on the surface is very low compared to the jet velocity. The low velocity results in a low transfer rate on the leeward surface.

When results for different hole diameters (d_i) are compared at a fixed outer boundary and Reynolds number, the area of uniform transfer coefficient increases with an increase in the active domain area on both the windward and the leeward surfaces. The flow velocity increases rapidly as the flow approaches the hole (roughly inversely proportional to the square of the distance, as in potential flow region). This rapid increase of velocity produces a rapid rise in the local mass transfer coefficient (Fig. 4). For the different d_o/d_i, the data collapse reasonably well when Sherwood number based on d_o-d_i is plotted against a dimensionless length scale, $(d-d_i)/(d_o-d_i)$ (Fig. 4). This implies that the characteristic length, d_o-d_i, can represent data with the absence of scale effects.

Data are also obtained from a square active domain (Fig. 2) to simulate results for a single hole in an array of holes. These data from the square domain are similar to those for the circular domain, since the flow field is axisymmetric at the single hole.

There are two representative characteristic lengths (d_o-d_i and d_o) for the Sherwood number on windward and leeward surfaces. At a given angle, the distance to the edge of the square domain can be compared to the annular radius, d_o-d_i. Since the Sherwood numbers for the square domain at $\theta = 0°$ are the same as those for the circular domain (Fig. 4) and the other angles for the square domain collapse onto the curve at $\theta = 0°$ [1], Sherwood number based upon (d_o-d_i) characterizes both circular and square domains. In general, a good characteristic length in a sink flow is the distance from the outer boundary to the inlet of the hole (d_o-d_i; a hydraulic diameter). The outer diameter, d_o, distance the center of the hole to the edge of the naphthalene boundary for both circular and square domains, is also a good characteristic length of windward surfaces for a fixed hole diameter with variable outer diameters [1].

Figure 5 shows local Sherwood numbers at various Reynolds numbers. The absence of data near the hole inlet is due to the metal rim around the hole inlet. The rim is necessary for measurements on the inside hole surface. The Sherwood number on the leeward surface is about one-third to one-half that on the windward surface and has a uniform value except near the outer edge (no data near the hole inlet). The averaged Sherwood numbers, obtained by the weighing measurements or by numerical integration of the local measurements, are plotted in Fig. 6 for various hole diameters and diameter ratios. The data for $d_o/d_i = 6.0$ from Gurdal's study, determined by a weighing mass transfer technique, compares well with the present data. Least-squares fits to the data are given by

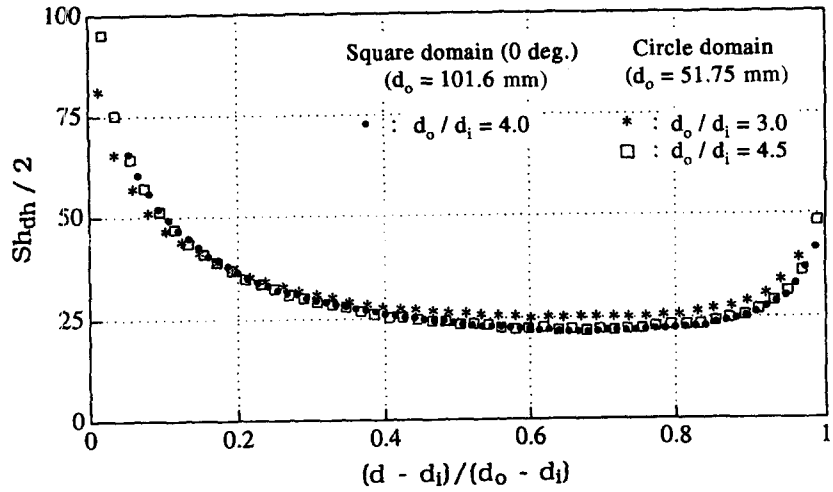

Fig. 4. Local Sherwood number based on d_h ($= d_o - d_i$) on the windward surface at $Re = 5000$.

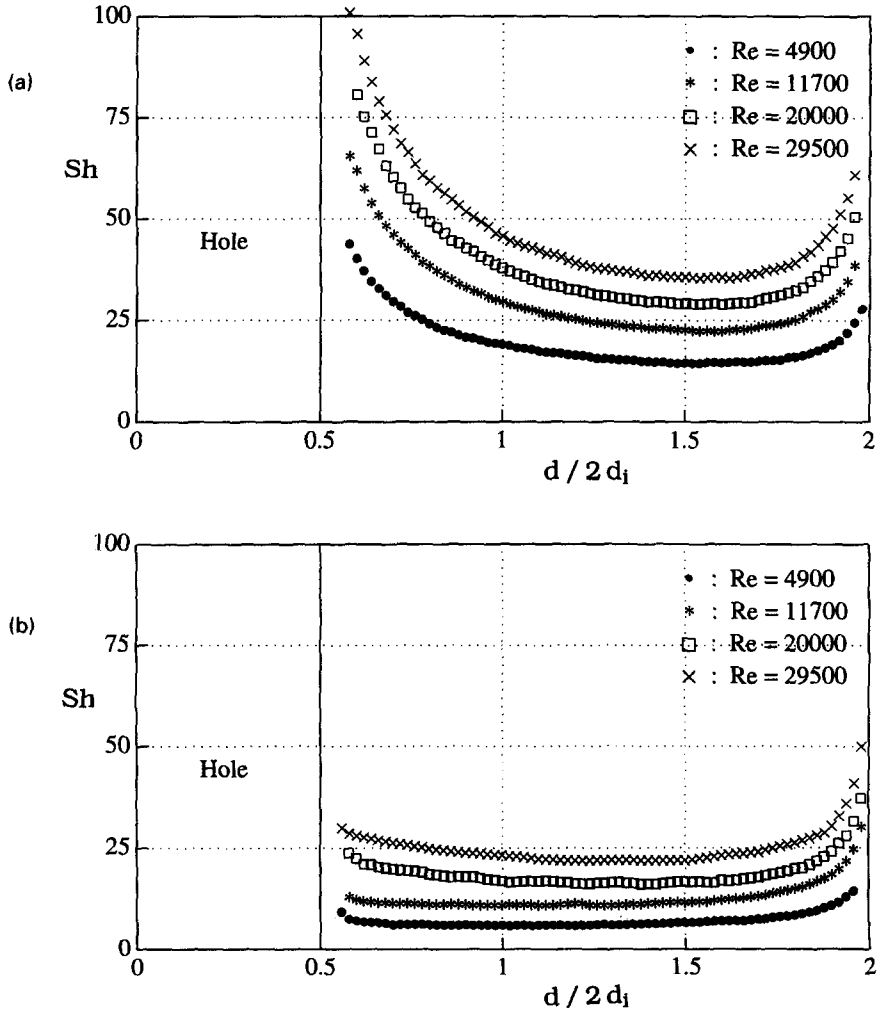

Fig. 5. Local Sherwood number at $d_i = 25.4$ mm: (a) windward surface; (b) leeward surface.

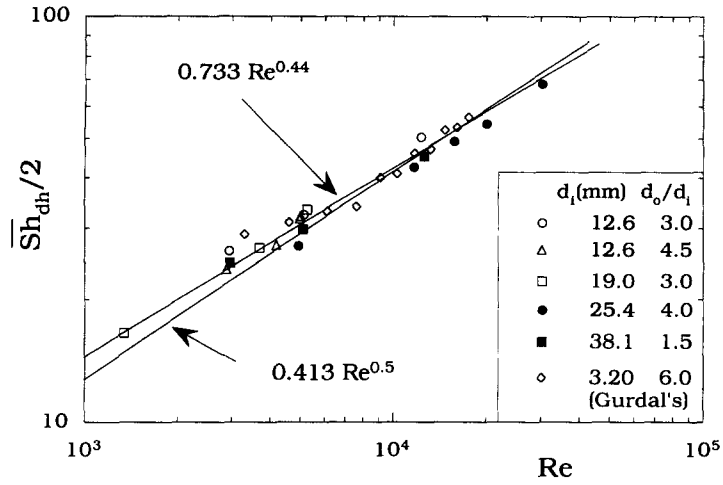

Fig. 6. Average Sherwood number on the windward surface (compared with Gurdal [3]).

$$\overline{Sh}_{dh}/2 = 0.733 Re^{0.44} \quad (3a)$$

$$\cong 0.413\, Re^{0.5}. \quad (3b)$$

This correlation (equation (3)), which the data fit within 6% deviation, is recommended for application in the range of $1.5 \leqslant d_o/d_i \leqslant 6.0$ and $1300 \leqslant Re \leqslant 30\,000$. However, the correlation might be extended to the wider ranges. The exponent of 0.44 is close to the 0.5 power of Reynolds number for laminar stagnation flow on a flat plate. The local Sh (in Fig. 5(a)) divided by $Re^{0.5}$ collapse well in a single curve for various Reynolds numbers [1]. This implies that the local Sh divided by $Re^{0.5}$ is almost independent of Reynolds number.

Inside hole surfaces

Figure 7 shows the local Sherwood number profiles at various Reynolds numbers in a range of $2000 \leqslant Re \leqslant 30\,000$. The inlet of the hole is located at $Y/d_i = 0$ and the exit at $Y/d_i = 1.48$. Each end of the injection hole has a circular rim for reference purposes. Thus there are no data at each end including the near region of the rims (i.e. measured data points are within $0.05 \leqslant Y/d_i \leqslant 1.42$).

According to the mass transfer pattern, the inside of the hole can be divided into three separate regions as shown in Fig. 3. They are

(A) the separation/recirculation region at the inlet of the hole;
(B) the reattachment region;
(C) the developing region.

The flow separates at the edge of inlet because the inlet is not a streamline-shape but has a sharp right-angled edge. The mass transfer coefficient in region A is usually low due to the recirculation and low velocity. The transfer coefficient increases rapidly in the reattachment region. Generally, the separation region near reattachment has a high turbulence level due to diffusion from the high shear stress generated at the mainstream/separation-bubble boundary. Lloyd and Brown [9] showed that a high turbulence region exists near the wall at $Y/d_i = 0.5$. Both the reattachment and the high turbulence are responsible for the increase in mass transfer in the vicinity $Y/d_i = 0.5$ (near reattachment). At low Reynolds number $Re = 2000$, there is no clear reattachment point (or clear peak in Sherwood number). A peak in the mass transfer rate is generally located just before the flow reattachment point.

When a laminar flow separates, the flow can change rapidly through transition and into turbulence. The following reattachment on the surface can be turbulent. Thus, a laminar separated flow can induce either laminar reattachment or turbulent reattachment flow. The approaching flow condition for the present study is laminar. The inlet flow remains laminar at the hole entrance due to strong acceleration.

The results are divided into two groups. A low Reynolds number ($Re \leqslant 3200$), the overall mass transfer rate is low where a laminar and weak reattachment with a long recirculation is expected. For $Re \geqslant 4900$, the high mass transfer occurs in the vicinity of a turbulent or transition reattachment point. The reattachment region has a high mass transfer rate because of the turbulence and the flow impingement on this region. The reattachment "line" will be a band rather than a line due to the unsteadiness of the flow. Goldstein *et al.* [13] and Eaton and Johnston [14] have shown for single step flows that with increasing Re the separation length increases in laminar flow, decreases rapidly in transition zone, and is nearly invariant in turbulent flow. Turbulent (or transition) flow reattachment in the hole is expected at Reynolds numbers higher than approximately $Re = 5000$. The separation length, actually the length from the inlet of the hole to the peak point of Sherwood number, has a minimum value at $Re = 8000$, increases slightly around $Re = 13\,000$, drops a little and then stays at a constant value of $Y_{peak}/d_i \cong 0.56$ (Fig. 7). This trend (increase

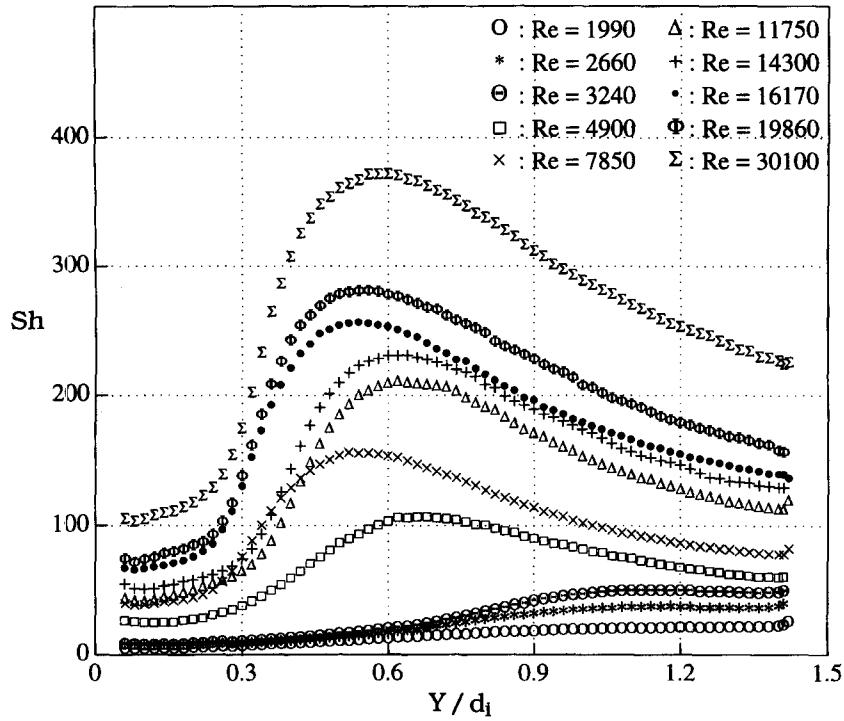

Fig. 7. Local Sherwood number inside the hole surface.

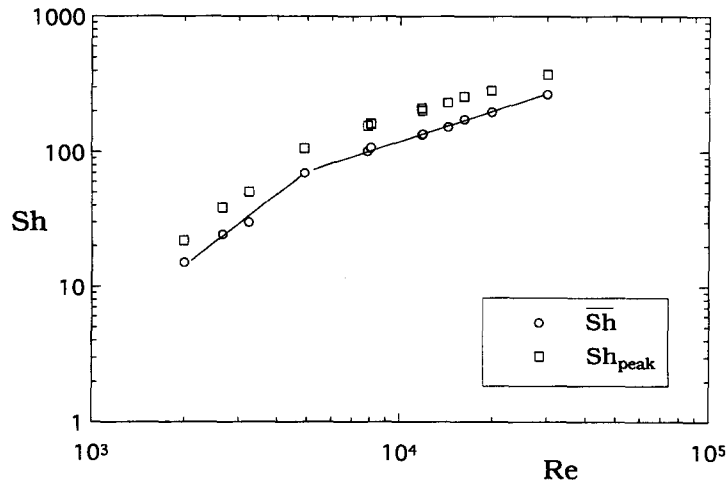

Fig. 8. Average and peak *Sh* inside the hole surface.

and decrease around $Re = 13000$) may be caused by the transition of the core flow in the hole. After reattachment, the boundary layers of velocity and concentration develop and the mass transfer coefficient decreases slowly, region *C* (Fig. 3).

The peak Sherwood number changes slope at $Re = 5000$ (Fig. 8). The average Sherwood number curve, found by numerically integrating the local data, is closely parallel to that for the peak values. The slope change might be caused by the transition of a laminar reattachment to a turbulent reattachment. The correlation equations, determined from least-squares fits are:

$$Sh_{peak} = 4.32 \times 10^{-5} Re^{1.7} \quad (Re \leqslant 5000) \tag{4a}$$

$$Sh_{peak} = 0.368 Re^{0.67} \quad (Re > 5000) \tag{4b}$$

$$\overline{Sh} = 4.10 \times 10^{-5} Re^{1.7} \quad (Re \leqslant 5000) \tag{5a}$$

$$\overline{Sh} = 0.167 Re^{0.72} \quad (Re > 5000) \tag{5b}$$

for $t/d_i = 1.48$.

Normalized heat/mass transfer coefficients inside a circular tube

The local transfer rates and the overall-averaged values of Sherwood number can be presented in a

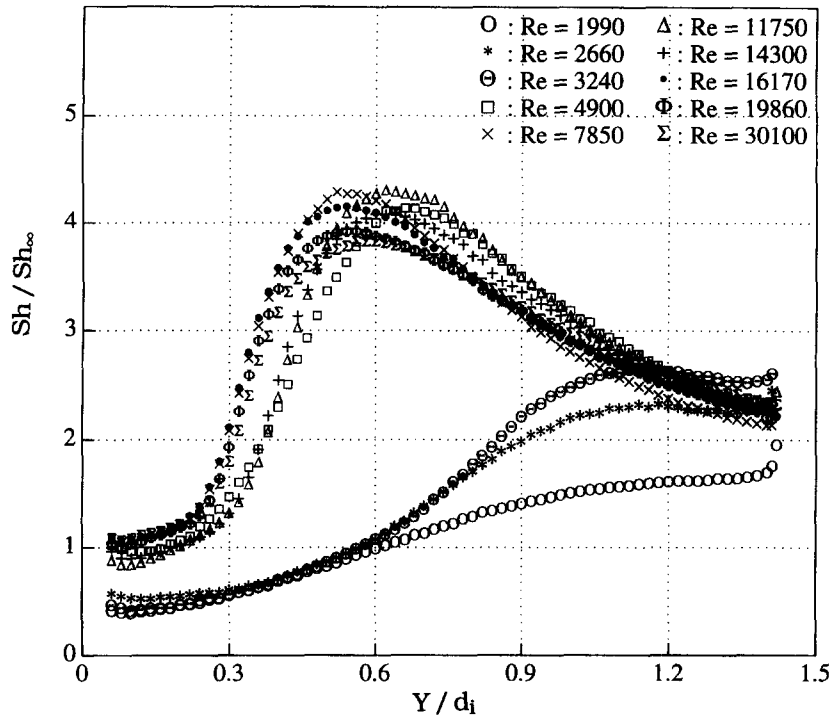

Fig. 9. Normalized *Sh* based on the transfer coefficient in a fully developed tube flow.

normalized form based on the transfer coefficient in a fully developed tube flow. Heat transfer correlations from a fully developed turbulent flow inside a circular tube have been presented in many studies. Mass transfer Sherwood numbers can be expressed in a form similar to that often used for the heat transfer Nusselt number:

$$Sh_\infty = C\,Re^m Sc^n. \tag{6}$$

The heat and mass transfer analogy indicates,

$$\frac{Nu_\infty}{Sh_\infty} = \left(\frac{Pr}{Sc}\right)^n. \tag{7}$$

The exponent n, is given as 0.33 in the correlation formula by Mills [6], 0.5 in the correlation formula by Kays and Crawford [15] and 0.4 in other correlations. The heat transfer correlations for fully developed tube flows have large differences (up to 20%) for $5000 \leqslant Re \leqslant 30\,000$. The fully developed (reference) Sherwood numbers are chosen from Mills' correlation, $Nu_\infty = 0.0397 Re^{0.73}\ Pr^{0.33}$, at least in part, because of the similarity to the Reynolds number exponent in equation (5b).

The normalized Sherwood numbers are shown in Fig. 9. The data for $Re \geqslant 4900$ collapse approximately onto a single curve and the values at the peak point are around four; that is, the local maximum coefficient of mass transfer is approximately four times the mass transfer coefficient in fully developed tube flow. In a different form, $(Sh - Sh_\infty)/(Sh_{peak} - Sh_\infty)$ vs Y/Y_{peak}, the data collapsed well to a single curve indicate that this normalized *Sh* is invariant with Reynolds number [1]. The peak Sherwood number and length can be determined from the correlation and graphs (equation (4) and Figs. 7 and 8).

The cumulatively-averaged values, Sh_L, which are an average from the entrance to the position L, are obtained for various Reynolds numbers (Fig. 10). For thin plates with $t/d_i \leqslant 0.6$, Sh_L should not be used to obtain the average Sherwood number. The mass transfer coefficient for such thin plates will be different as no reattachment occurs, and a recirculating zone extends to the leeward side. The cumulatively-averaged values, normalized by the fully developed coefficient, may be divided into two groups, laminar and turbulent reattachments. The Sh_L values for $Re < 4900$ are less than 2.0. The peak values of Sh_L for $Re \geqslant 4900$ are around 2.8 to 3.0. The peak value of approximately 2.9 is slightly higher than the cumulatively-averaged peak value of 2.64 obtained, for a long tube with a right angle edge, Mills [6]. A correlation curve is fitted by the present data and matching to Mills' data at a large Y/d_i. The equations are given by:

for $0.6 \leqslant Y/d_i \leqslant 1.5 (L = Y/d_i)$

$$\frac{Sh_L}{Sh_\infty} = -1.016 + 16.68L - 22.48L^2 + 12.93L^3 - 2.775L^4 \tag{8a}$$

and for $1.5 < Y/d_i \leqslant 10$ $(L = Y/d_i)$

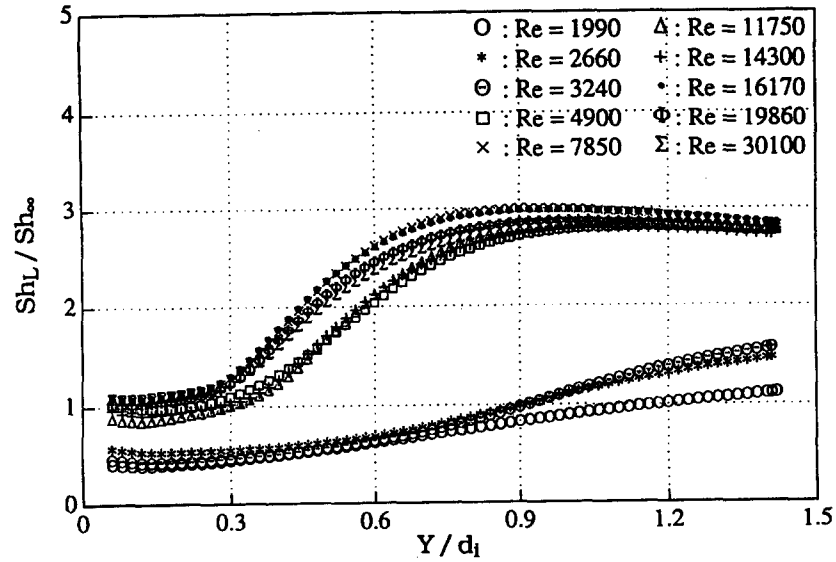

Fig. 10. Normalized cumulatively-averaged *Sh* inside the hole surface.

$$\frac{Sh_L}{Sh_\infty} = 1.0+6.843\left(\frac{1}{L}\right)-15.99\left(\frac{1}{L}\right)^2 +24.55\left(\frac{1}{L}\right)^3-15.06\left(\frac{1}{L}\right)^4 \approx 1.0+\frac{2.384}{L^{0.621}}. \quad (8b)$$

The data collapse better on a single curve in a Sh_L/Sh_∞ vs Y/Y_{peak} plot [1]. The correlation equation can be converted to

$$\frac{Sh_L}{Sh_\infty} = -2.603 +9.308L'-5.863L'^2+1.637'^3-1.746L'^4 \quad (9)$$

for $1.0 \leqslant Y/Y_{peak} \leqslant 2.5$ $(L' = Y/Y_{peak})$.

Comparison of the individual surfaces and average transfer coefficients

The mass transfer coefficient variation on the surfaces is compared for the various Reynolds numbers for $d_o = 4d_i$ and $t/d_i = 1.48$ in Fig. 11. The transfer coefficient on the inside hole surface predominates and the coefficient at the leeward surface is quite small (about 14% of the total mass transfer). Although the inside hole surface is only 16.5% of the total active area, about 60% of the total mass transfer takes place from it.

Figure 12 shows the overall-averaged mass transfer coefficients (the hole and plates combined) for various hole diameters, d_i, the diameter ratios, d_o/d_i and the plate thickness ratios, t/d_i. A reasonable correlation using three equations which may correspond to laminar, transition and turbulent flows would be,

$$\overline{\overline{Sh}}_{do} = 1.6780Re^{0.426} \quad (Re \leqslant 2000) \quad (10)$$

$$\overline{\overline{Sh}}_{do} = 0.0388Re^{0.915} \quad (2000 < Re \leqslant 5000) \quad (11)$$

$$\overline{\overline{Sh}}_{do} = 0.4326Re^{0.633} \quad (5000 < Re \leqslant 30\,000). \quad (12)$$

CONCLUSIONS

Local mass transfer coefficients for flow through short single circular holes are detailed in this study using the naphthalene sublimation technique. The measurements focus on the inside hole surface as well as the near region on the windward and leeward surfaces outside the hole.

(i) At the windward surface, the local transfer coefficient increases rapidly as the flow approaches the hole entrance due to acceleration of the flow resulting in a thinning boundary layer. Increasing the area of the active domain results in a relatively minor increase in the total mass transfer.

(ii) Use of the characteristic length of (d_o-d_i), which is the distance from the outer boundary (active area) to the edge of the hole, collapses the data on a single curve for various dimensions of windward surfaces. Mass transfer rate increases with Reynolds number raised to the 0.5 power.

(iii) For the leeward surface, the mass transfer is very low due to a low entrainment velocity on the surface compared to the exit jet velocity. The overall transfer rate is, for example, only about 14% of the total rate even though this surface contains about 42% of the active surface area.

(iv) Inside the hole, a separation zone present near the hole entrance decreases with increasing Reynolds number up to $Re = 5000$. For $Re \geqslant 5000$, the separation zone reaches a minimum size (approximately $0.56d_i$) and is changed little with Reynolds number (turbulent reattachment).

(v) The peak *Sh* near reattachment is about four

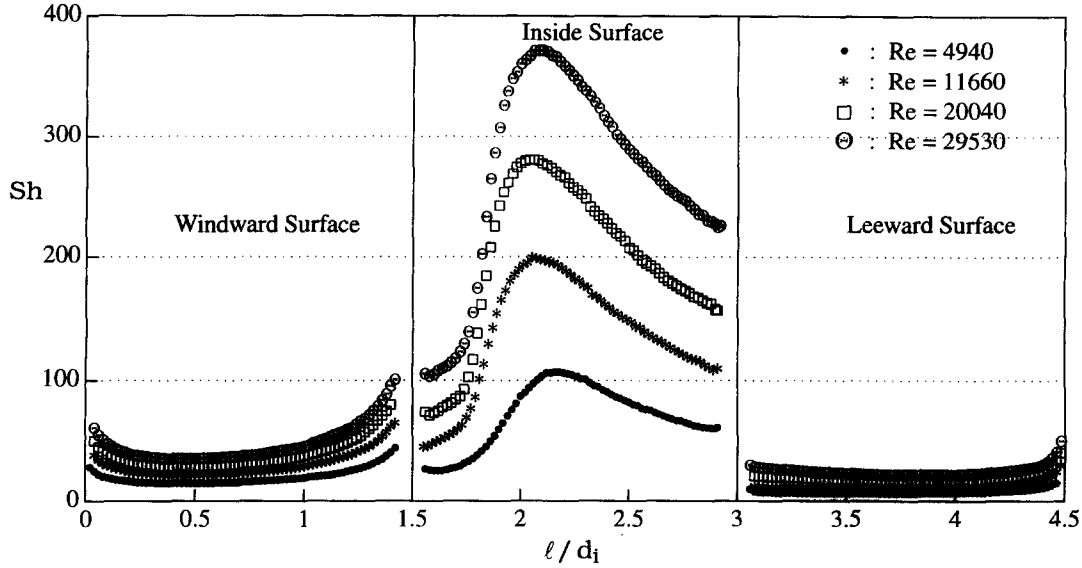

Fig. 11. Comparison of local *Sh* for a single hole.

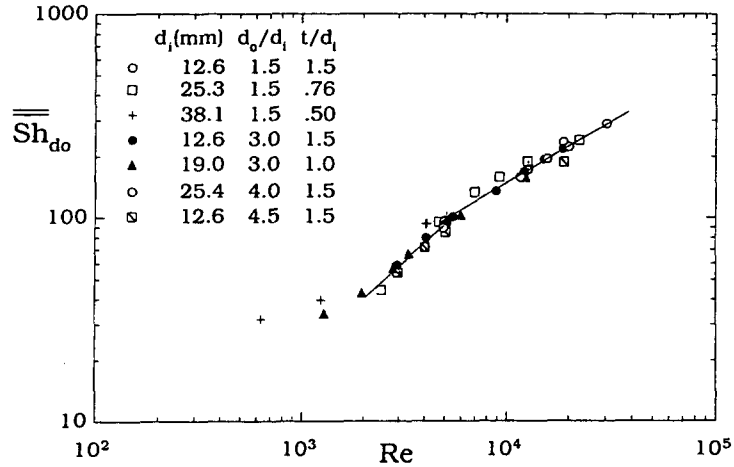

Fig. 12. Overall-averaged Sherwood numbers based on the diameter of outer (active) boundary, d_o.

times that in a fully developed tube flow. The normalized Sherwood number data based on the fully developed value (Sh/Sh_∞) collapse onto a single curve for $Re \geqslant 5000$. Thus, the correlation equation can be used over a range of Reynolds number.

(vi) Use of the diameter of the outer boundary (active area), d_o, as a characteristic length brings the overall-averaged Sherwood number together on a single curve for different d_i, d_o/d_i, t/d_i and *Re*.

Acknowledgement—Support from the Air Force Office of Scientific Research and the Department of Energy AGTS program greatly aided the conduct of this study.

REFERENCES

1. Cho, H. H., Heat/mass transfer flow through an array of holes and slits. Ph.D. thesis, University of Minnesota, Minneapolis, MN, 1992.
2. Cho, H. H. and Goldstein, R. J., Heat (mass) transfer and film cooling effectiveness with injection through discrete holes—part I: within holes and on the back surface. *Journal of Turbomachinery*, 1995, **117**, 440–450.
3. Gurdal, U., Heat transfer at an upstream-facing surface washed by fluid en route to an aperture in the surface. M.S. thesis, University of Minnesota, Minneapolis, MN, 1980.
4. Lichtarowicz, A., Duggins, R. K. and Markland, E., Discharge coefficients for incompressible non-cavitating flow through long orifices. *Journal of Mechanical Engineering Science*, 1965, **7**, 210–219.
5. Boelter, L. M. K., Young, G. and Iversen, H. W., Distribution of heat-transfer rate in the entrance section of a circular tube. *NACA TN*—1451, 1948.
6. Mills, A. F., Experimental investigation of turbulent heat transfer in the entrance region of a circular conduit. *Journal of Mechanical Engineering Science*, 1962, **4**, 63–77.
7. Petukhov, B. S., Heat transfer and friction in turbulent pipe flow with variable physical properties. In *Advances in Heat Transfer*, Vol. 6, ed. J. P. Hartnett and T. F. Irvine. Academic Press, New York, 1970, pp. 503–564.

8. Al-Arabi, M., Turbulent heat transfer in the entrance region of a tube. *Heat Transfer Engineering*, 1982, **3,** 76–83.
9. Lloyd, S. and Brown, A., Fluid flow and heat transfer characteristics in the entrance region of circular pipes. *ASME paper* 85-*GT*-121, 1985.
10. Goldstein, R. J. and Cho, H. H., A review of mass transfer measurements using naphthalene sublimation. *Experimental Thermal and Fluid Science*, 1995, **10,** 416–434.
11. Ambrose, D., Lawrenson, J. and Sparke, C. H. S., The vapor pressure of naphthalene. *Journal of Chemical Thermodynamics*, 1975, **7,** 1173–1176.
12. Kline, S. J. and McClintock, F. A., Describing uncertainty in single-sample experiments. *Mechanical Engineering*, 1953, **75,** 3–8.
13. Goldstein, R. J., Eriksen, V. L., Olson, R. M. and Eckert, E. R. G., Laminar separation, reattachment and transition of the flow over a downstream-facing step. *Journal of Basic Engineering*, 1970, **92,** 732–741.
14. Eaton, J. K. and Johnston, J. P., A review of research on subsonic turbulent flow reattachment. *AIAA Journal*, 1981, **19,** 1093–1100.
15. Kays, W. M. and Crawford, M. E., *Convective Heat and Mass Transfer*. McGraw-Hill, New York, 1994.